의학박사 학위논문

Periostin Induces Kidney Fibrosis after Acute Kidney Injury via p38 MAPK pathway

Periostin이 급성신손상 후 신 섬유화에 미치는 영향

2018 년 2 월

서울대학교 대학원

임상의과학과

안 정 남

Abstract

Periostin Induces Kidney Fibrosis after Acute Kidney Injury via p38 MAPK pathway

Jung Nam An
Department of Clinical Medical Sciences
The Graduate School
Seoul National University

Background: Periostin, a matricellular protein, has been reported to play a crucial role in fibrosis. Acute kidney injury results in a high risk of progression to chronic kidney disease. It was hypothesized that periostin is involved in the progression of acute kidney injury to kidney fibrosis.

Methods: Unilateral ischemia-reperfusion injury using 7- to 8-week-old male wild-type and *periostin null* mice was induced and the animals were observed for 6 weeks. *In vitro,* human kidney-2 cells were subjected to a hypoxic incubator (5% O_2, 5% CO_2, and 90% N_2) for 24 hours and 5 days. The cells were also cultured with a p38 mitogen-activated protein kinase (MAPK) inhibitor in the hypoxic incubator for 5 days.

Results: At 6 weeks after induction of unilateral ischemia-reperfusion injury, the kidneys in *periostin null* mice were less atrophied, and interstitial fibrosis/tubular atrophy was significantly alleviated in *periostin null* mice compared with those in wild-type mice. The expressions of phosphorylated-p38 MAPK were also decreased in *periostin null* mice

compared to those in wild-type mice. Furthermore, *periostin null* mice had attenuated mRNA and protein expression of fibrosis and apoptosis markers. *In vitro,* hypoxic injury (5% O_2, 5% CO_2, and 90% N_2) of the human kidney-2 cells for 24 hours and 5 days increased the expressions of phosphorylated-p38 MAPK and fibrosis markers. Recombinant periostin in hypoxic conditions enhanced phosphorylated-p38 MAPK expression, which was comparable to that with recombinant transforming growth factor-β1. In contrast, inhibition of p38 MAPK ameliorated hypoxia-induced fibrosis.

Conclusion: In conclusion, periostin promotes kidney fibrosis via the p38 MAPK pathway following acute kidney injury triggered by hypoxic or ischemic insult. Periostin ablation could protect against kidney progression.

Keywords: periostin, acute kidney injury, kidney fibrosis, hypoxia, *periostin null* mice, unilateral ischemia-reperfusion injury, p38 mitogen-activated protein kinase

Student Number: 2014-30912

Contents

Abstract 1
Contents 3
List of figures 4
Introduction 5
Materials and Methods 7
Results 12
Discussion 29
Reference 33
Abstract (Korean) 38

List of Figures

Figure 1 13
Figure 2 16
Figure 3 18
Figure 4 21
Figure 5 25

Introduction

Periostin, a matricellular protein, is associated with normal development of teeth, bone, heart, and kidney during the embryonic period [1-3], but thereafter, its expression has been associated with congestive heart failure [4, 5], myocardial infarction [6, 7], muscle injury, asthma [8], and development and metastasis of various malignancies [9-11]. In addition, previous clinical and experimental studies have reported that periostin was highly expressed in fibrotic tissues [12, 13] and associated with disease severity in several chronic kidney disease (CKD) models such as diabetic nephropathy or hypertensive nephropathy [14].

Periostin primarily binds to integrin, and crosstalk with receptor tyrosine kinases, such as epidermal growth factor receptor in the plasma membrane, is observed. Then, it activates the AKT- or FAK-mediated signaling pathway and regulates various cell functions, including cell adhesion, mobility, migration, survival, proliferation, and angiogenesis [15]. Moreover, is binds extracellular matrix molecules, such as collagen IV and fibronectin, which leads to extracellular matrix remodeling, organization, fibrillogenesis, and epithelial-mesenchymal transition [16-18].

Acute kidney injury (AKI) occurs in 5-10% of hospitalized patients and in more than 30% of critically ill patients [19]. The incidence of AKI has increased every year [19], which has major direct and indirect clinical implications. AKI results in impeded treatment for comorbidities, increased risk of acute renal replacement therapy, longer hospital stays, increased burden of medical costs, and increased mortality rates (up to 50-80%) [20, 21].

Furthermore, AKI patients showed a higher risk of progression to CKD [22], which was substantial when the AKI patients experienced more episodes and more severe injury [23, 24]. Recently, it was reported that

severe AKI patients requiring continuous renal replacement therapy (CRRT) had a greater risk of progression to end-stage renal disease compared to that of stage 3 CKD patients who did not undergo an AKI episode, even if their renal function recovered at 3 months [25].

Similarly, periostin plays a crucial role in the fibrosis in diverse organs, including the kidney; however, the association between the progression of AKI to CKD and periostin has not been investigated. In the present study, a "progression of AKI to CKD model" was established and the effects of periostin were analyzed. Then, whether the inhibition of periostin was a protective factor for progression of AKI to CKD were investigated.

Materials and Methods

Experimental animals

Male wild-type (WT) mice (C57BL/6; B6) were purchased from Koatech (Seoul, Korea) and male *periostin* (*Postn*) *null* mice (*Postn*$^{-/-}$) (B6;129-*Postn*^{tm1Jmol}/J) [26] were purchased from the Jackson Laboratory (Bar Harbor, ME, USA). All of the 7- to 8-week-old mice used in the experiments were raised in a specific pathogen-free animal facility. All experiments were performed under the approval of the Institutional Animal Care and Use Committee of Clinical Research Institute at Seoul National University Boramae Medical Center (2016-0001) and in accordance with the Guidelines for the Care and Use of Laboratory Animals of the National Research Council and the NIH guide for the Care and Use of Laboratory Animals.

Establishment of progressive kidney injury in vivo model

A “progression of AKI to CKD model” was designated as the “progressive kidney injury model”. Firstly, to establish a progressive kidney injury *in vivo* model, unilateral ischemia-reperfusion injury (UIRI) was induced in the left kidney pedicle for 30 minutes in WT mice and *Postn null* mice. The mice were anesthetized with xylazine (Rompun; 10 mg/kg; Bayer, Canada) and tiletamine mixed with zolazepam (1:1) (Zoletil^{TM}; 30 mg/kg; Virbac, USA). After unilateral flank incision, the left renal pedicle was cross-clamped for 30 minutes with microaneurysm clamps (Roboz Surgical Instrument Co., Gaithersburg, MD), and then, reperfusion was performed. During the procedure, pre-warmed (37°C) PBS (500 μl) was administered intraperitoneally for optimal fluid balance, and the animals were placed on a heating pad (37°C). Sham-operated mice received the same

surgical procedure except for the clamping of renal pedicle. After 6 weeks, mice were sacrificed, and blood, urine, and kidney tissues were obtained. Gross features and the weights of both kidneys were examined, and the weight ratios of left kidney to right kidney were analyzed.

Establishment of progressive kidney injury in vitro model

For the progressive kidney injury *in vitro* model, a "hypoxia induced fibrosis" experiment was performed. The human kidney-2 (HK-2) cell line (ATCC® CRL-2190™, Manassas, Virginia, USA), an immortalized proximal tubule epithelial cell line, was used. The cells were incubated in DMEM/F12 medium and cultured on petri dishes (BD Biosciences, Franklin Lakes, NJ, USA) until colonies were established, and passages 2 to 3 were used in this study. Then, HK-2 cells (2×10^5/well) were plated into a 6-well plate. After starvation in serum-free media for 24 hours, HK-2 cells were incubated with recombinant transforming growth factor-beta1 (rTGF-β1, 2 ng/mL) at 21% O_2, 5% CO_2, and 74% N_2, which was used as a positive control. For hypoxia induction, HK-2 cells also were subjected to a hypoxic incubator (5% O_2, 5% CO_2, and 90% N_2). Under this condition, after 24 hours, the expression of phosphorylated p38 mitogen-activated protein kinase (phospho-p38 MAPK) was observed as an acute response of hypoxia; then, fibrosis was induced via hypoxia injury for 5 days. Moreover, to assess the protective effect on fibrosis, the cells were pre-treated for 1 hour and cultured with a p38 MAPK inhibitor (SB-731445) [27], supplied by GSK Global (Hertfordshire, UK), at concentrations of 1 and 2 μM, in the hypoxic incubator for 5 days.

Histological analyses

For histological analyses, 4 μm-thick paraffin sections were stained with Masson's trichrome and Sirius red. For immunohistochemistry assays,

paraffin-embedded kidneys cut into 4 μm-thick slices were deparaffinized and hydrated using xylene and ethanol. Endogenous biotin activity was blocked by 3% hydrogen peroxide. Deparaffinized sections were stained with anti-collagen 1A1 antibody (Abcam, Cambridge, MA, USA), anti-S100A4 antibody (Abcam), anti-cleaved caspase-3 antibody (Cell Signaling, Danvers, MA, USA), or anti-phospho-p38 MAPK antibody (Cell Signaling), and then incubated with HRP-conjugated goat anti-rabbit IgG (Vector Laboratories, Burlingame, CA, USA). The 3, 3'-diaminobenzidine tetrahydrochloride (Sigma-Aldrich, Saint Louis, MO, USA) were used for immunhistochemical detection. Finally, all sections were counterstained with Mayer's hematoxylin (Sigma-Aldrich) and evaluated under light microscopy. For each sample, 5 fields (100× magnification) were assessed for positive staining (%) by a morphometry system (Qwin 3, Leica, Netherlands).

Confocal microscopic examination

To detect the expression of phospho-p38 MAPK, the sections were stained with anti-phospho-p38 MAPK antibody (Cell Signaling) in a blocking reagent overnight at 4°C. A second layer of Alexa Fluor® 555-conjugated goat anti-rabbit antibody (Molecular Probes, Eugene, OR, USA) was applied and incubated at room temperature for one hour. All sections were washed and then incubated for an additional 5 minutes with 4', 6-diamidino-2-phenylindole (DAPI, Molecular Probes) for counterstaining. For the negative controls, primary antibody was omitted from sections. Sections were blindly and randomly evaluated, and images were captured using a Leica TCS SP8 STED CW (Leica, Mannheim, Germany) and MetaMorph version 7.8.10 software (Universal Imaging, Downingtown, PA).

For *in vitro* studies, HK-2 cells cultured with rTGF-β1 (2 ng/mL) or recombinant periostin (rPeriostin) (1000 ng/mL; R&D systems, Minneapolis, MN, USA) were incubated. After 24 hours, immunofluorescence staining was

performed for DAPI and phospho-p38 MAPK. The proportions of phospho-p38 MAPK-positive cells were assessed for quantitative analysis.

Quantitative real-time PCR

Total RNA was isolated from mouse kidney tissues 6 weeks after disease induction, and the mRNA levels were analyzed by real-time PCR. Briefly, 1 μg of total RNA extracted using the RNeasy kit (Qiagen GmBH, Hilden, Germany) was reverse-transcribed using oligo-d(T) primers and AMV-RT Taq polymerase (Promega, Madison, WI, USA). Real-time PCR was performed using either an Assay-on-Demend TaqMan probes or the SYBR Green method and primers for α-smooth muscle actin (α-SMA), fibronectin, collagen 1A1, periostin, TGF-β1, p53, caspase-9, glycogen synthase kinase 3β (GSK3β), p38 MAPK, and glyceraldehyde-3-phosphate dehydrogenase (GAPDH) (Applied Biosystems, Foster City, CA, USA) with an ABI PRISM 7500 Sequence Detection System. Relative quantification was done using the ΔΔCT method. The mRNA expression levels were normalized using the GAPDH mRNA expression.

Western blot analyses

Kidney tissues were harvested from mice 6 weeks after disease induction, and cells were collected 5 days after the establishment of the *in vitro* model. After protein extraction from tissues and cells, equal amounts (80 μg) were separated on 10% sodium dodecyl sulfate (SDS)-polyacrylamide gels and transferred onto Immobilon-FL 0.4 μM polyvinylidene difluoride membranes (Millipore, Bedford, MA, USA). Primary antibodies targeting β -actin (Sigma-Aldrich), fibroblast-specific protein-1 (FSP-1), α-SMA, E-cadherin, fibronectin, B-cell lymphoma 2 (Bcl-2), collagen 1A1, periostin, and snail (Abcam) were used. Anti-mouse IgG and anti-rabbit IgG (Vector Laboratories) was used as secondary antibodies. The target molecule

expression levels were normalized with respect to the amount of β-actin expression. Densitometry was performed using the gel analysis process of ImageJ software (National Institutes of Health, Bethesda, Maryland, USA). After densitometric analyses of various markers in all tissue and cellular samples, only representative samples were shown in the figures.

Statistics

The results are expressed as the mean ± standard deviation or the median (interquartile ranges) based on the results of the Shapiro-Wilk normality test. Student's t-test or the Mann-Whitney U test was used according to their normality. For comparison of more than two groups, one- or two-way ANOVA using Tukey's test was performed. Statistical analyses were performed using SPSS version 22 (IBM software, USA) and GraphPad Prism 5.0 (GraphPad Software, Inc., San Diego, CA, USA). Statistical significance was determined at $P < 0.05$.

Results

In the progressive kidney injury model, fibrosis was attenuated in periostin null mice.

To determine the role of periostin in the progression of AKI to kidney fibrosis (designated as "progressive kidney injury"), UIRI was induced in WT mice and *Postn null* mice and the animals were observed for 6 weeks.

After 6 weeks of disease induction, the left kidneys of WT mice were shrunk and smaller in weight than those in the sham group. However, the left kidneys in *Postn null* mice were significantly less atrophied and larger in weight compared to those of WT mice (WT UIRI *vs.* *Postn null* UIRI, 0.30 ± 0.05 *vs.* 0.50 ± 0.17; $P = 0.004$) (**Figure 1A**).

Consistent with these findings, WT mice exhibited more prominent histological changes, including tubular atrophic changes, interstitial fibrosis, and collagen fiber deposition, compared with those of control mice. In contrast, the pathologic changes of *Postn null* mice kidneys were less extensive than those of the WT mice (**Figure 1B**). The expressions of collagen 1A1 (WT UIRI *vs.* *Postn null* UIRI, 24.96 ± 1.46 *vs.* 17.10 ± 3.09; $P = 0.012$) and S100A4 were also significantly alleviated in *Postn null* mice compared with those in WT mice.

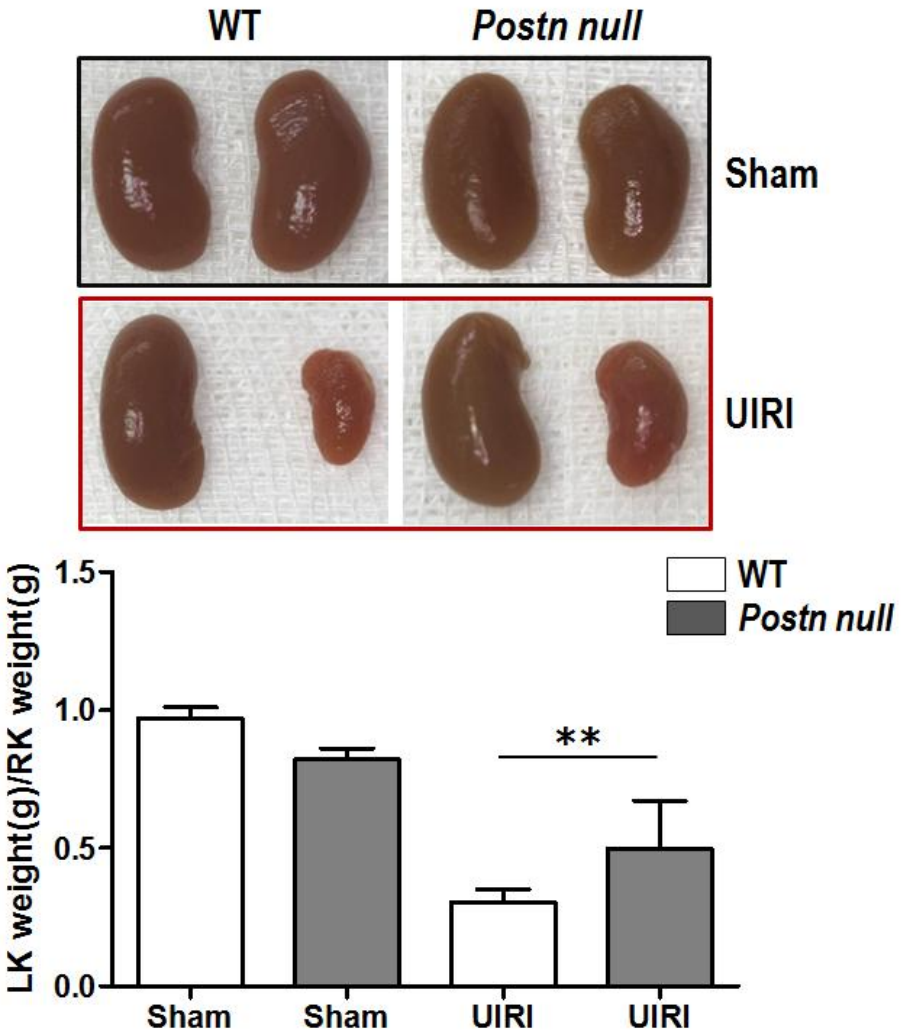

Figure 1. In progressive kidney injury model, fibrosis was attenuated in *periostin null* mice. (A) Gross features and kidney weights after 6 weeks of disease induction. At 6 weeks after disease induction, the left kidneys of *Postn null* mice were significantly less atrophied and weighted more compared to those of WT mice (n = 8/group; $^{**}P < 0.01$).

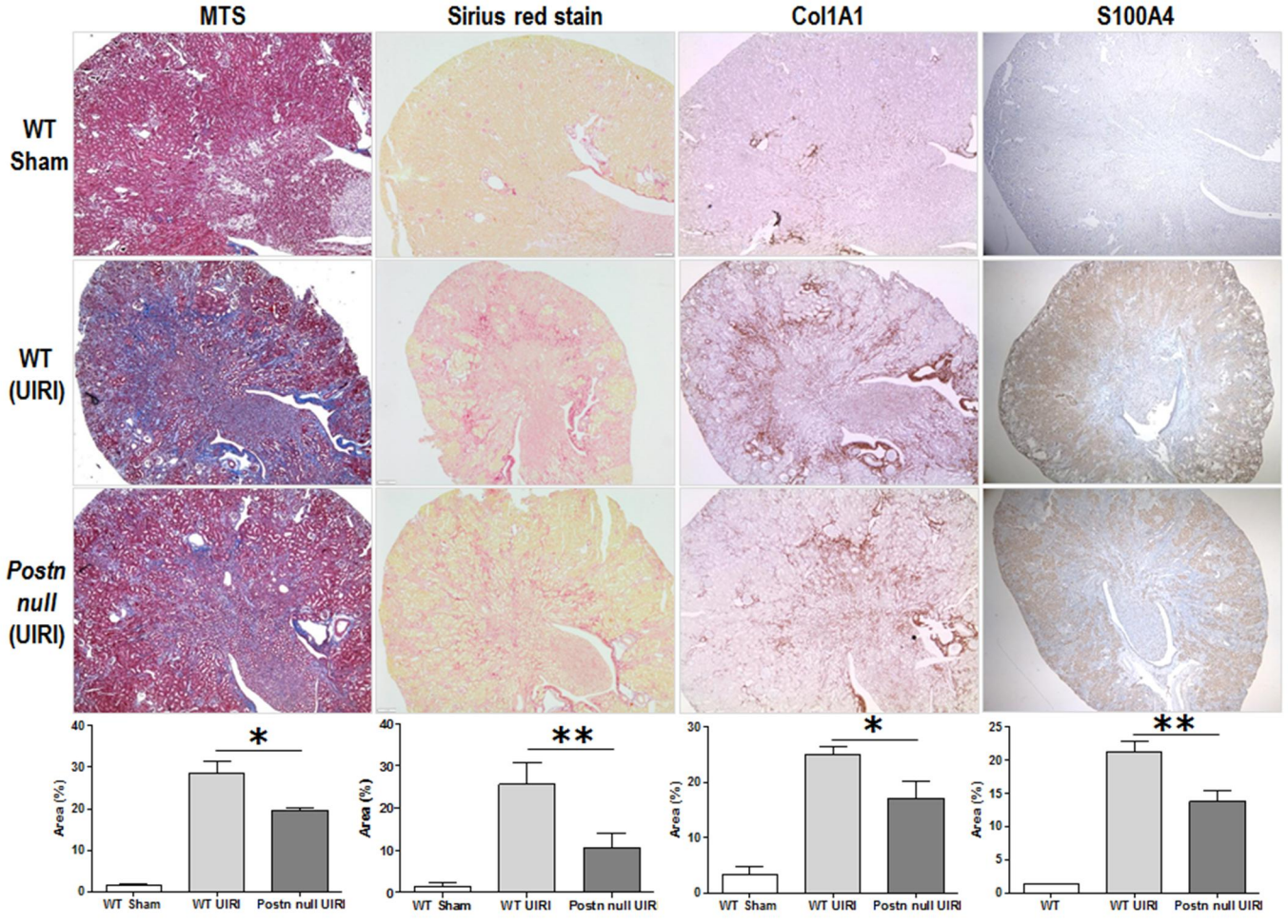
MTS
Sirius red stain
Col1A1
S100A4
WT Sham
WT (UIRI)
Postn null (UIRI)
Area (%)
WT Sham
WT UIRI
Postn null UIRI
WT
*
**

(B) Masson's trichrome stain, sirius red stain, and immunohistochemistry of fibrosis markers. *Postn null* mice showed less extensive pathologic changes and expressions of collagen 1A1 and S100A4 compared with those of the WT mice (n = 8/group; $*P < 0.05$, $**P < 0.01$; magnification: ×40). Data are shown as mean ± standard deviation and Student's t-test was used. These results represent one of three independent experiments.

Similar to the histological and clinical changes, the mRNA expressions of several fibrosis markers, such as α-SMA, fibronectin, collagen 1A1, TGF-β1, and periostin (WT sham *vs.* WT UIRI 1.18 ± 0.60 *vs.* 58.15 ± 97.64; $P < 0.001$), were significantly elevated in WT mice compared to those in control mice and were prominently attenuated in *Postn null* mice (**Figure 2A**).

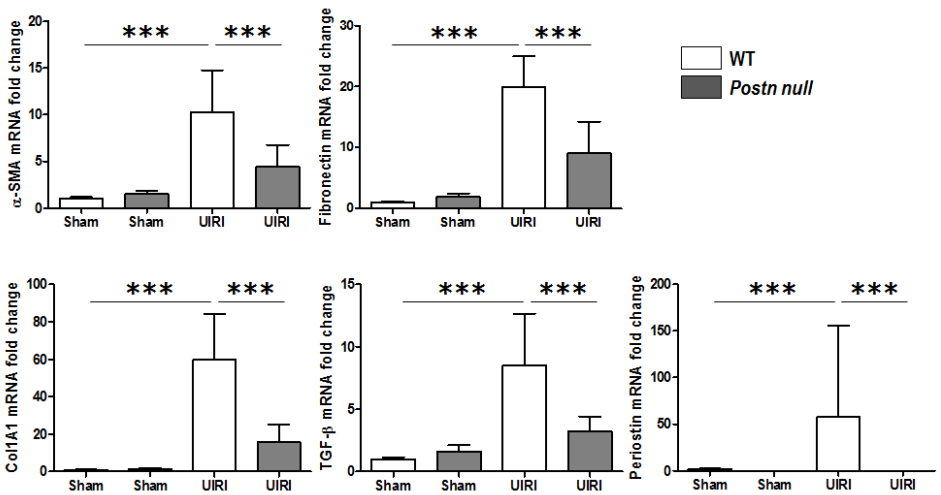

Figure 2. Intrarenal expressions of fibrosis markers in the progressive kidney injury model. (A) The mRNA levels of fibrosis markers. In real-time PCR, the expressions of various fibrosis markers, including α-SMA, fibronectin, collagen 1A1, TGF-β1, and periostin, were significantly elevated in WT mice compared to those in control mice and were significantly attenuated in *Postn null* mice (n = 10/group; ***$P < 0.001$).

In addition, western blot analyses of all tissue protein samples were performed and the band densities were analyzed. The results of representative samples are shown in **Figure 2B**. The results also indicated that the expressions of α-SMA and FSP-1 were greater in WT mice than those in *Postn null* mice, whereas E-cadherin expression significantly increased in *Postn null* mice compared to that in WT mice.

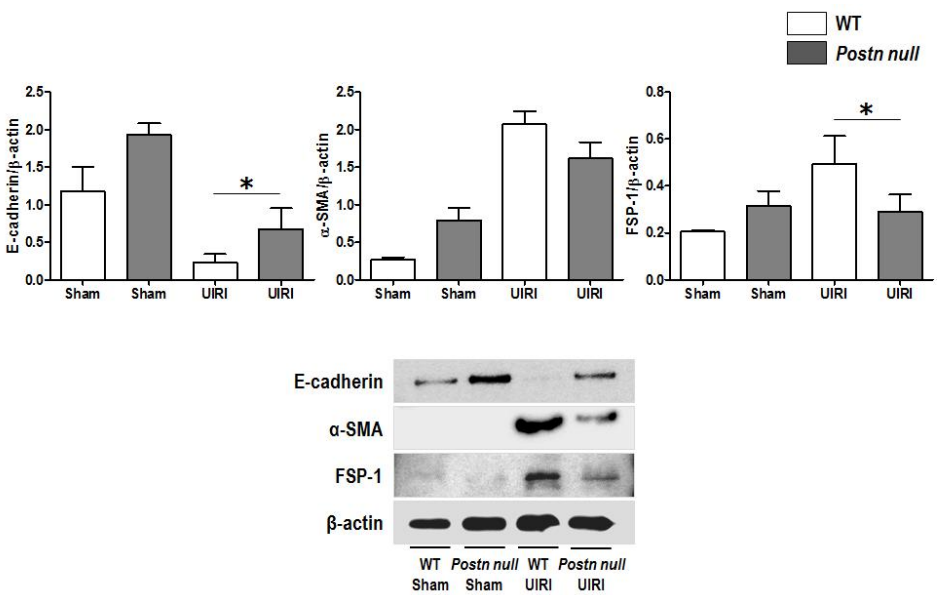

(B) The protein levels of fibrosis markers. In densitometry analyses of western blot results and the results of representative samples, the expressions of α-SMA and FSP-1 were substantially elevated in WT mice compared to that in control mice and were significantly attenuated in *Postn null* mice. In contrast, E-cadherin was prominently expressed in *Postn null* mice rather than in WT mice (n = 10/group; $*P < 0.05$). Data are shown as mean ± standard deviation and Student's t-test was used. These results represent one of three independent experiments.

In the progressive kidney injury model, apoptosis was decreased in periostin null mice.

Firstly, to verify the relationship between progressive kidney injury and apoptosis, the expression of cleaved caspase-3 was examined in the kidney tissues 6 weeks after disease induction (**Figure 3A**). The highly expressed cleaved caspase-3 in WT mice was significantly decreased in *Postn null* mice.

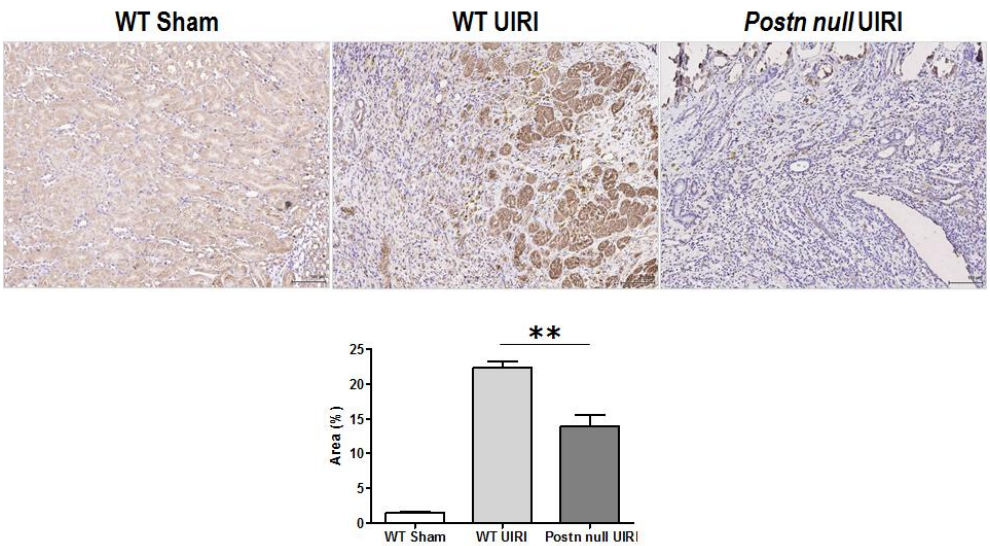

Figure 3. In the progressive kidney injury model, apoptosis was decreased in *periostin null* mice. (A) The expression of cleaved caspase-3. The expression of cleaved caspase-3 in kidney tissues 6 weeks after disease induction was significantly decreased in *Postn null* mice compared to that in WT mice (n = 8/group; $^{**}P < 0.01$; magnification: ×200).

Next, mRNA and protein levels of apoptosis markers were quantified using real-time PCR and western blot analyses (**Figure 3B**). Caspase-9, GSK3β, and p53 (WT sham *vs.* WT UIRI *vs. Postn null* UIRI 1.00 ± 0.09 *vs.* 2.77 ± 0.92 *vs.* 1.44 ± 0.67; $P < 0.001$) substantially increased in WT mice along with the development of progressive kidney injury compared to those in *Postn null* mice. In contrast, the expression of Bcl-2 was higher in *Postn null* mice than that in WT mice.

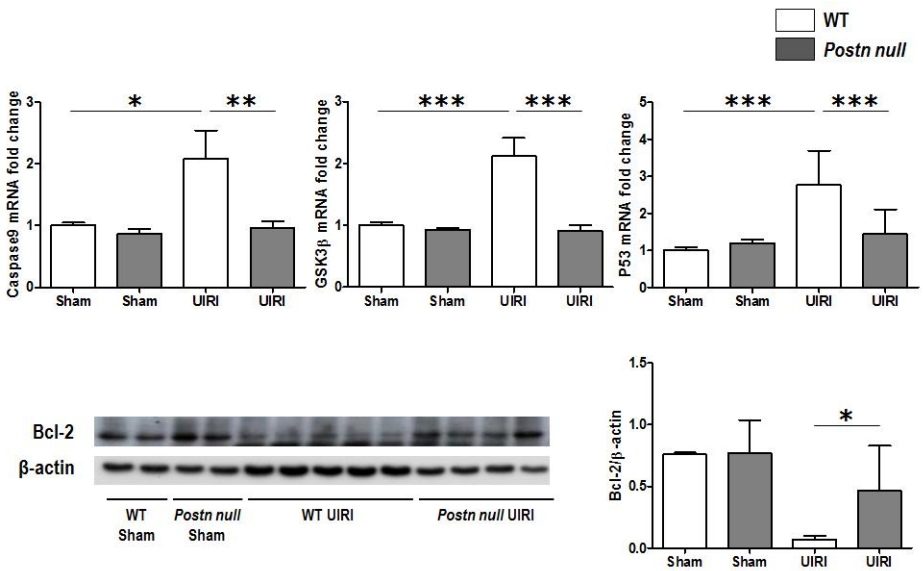

(B) The mRNA and protein levels of apoptosis markers. Caspase-9, GSK3β, and p53 were significantly increased in WT compared to those in *Postn null* mice; however, Bcl-2 was higher in *Postn null* mice than that in WT mice (n = 10/group; **P* < 0.05, ***P* < 0.01, ****P* < 0.001). Data are shown as mean ± standard deviation and Student's t-test was used. These results represent one of three independent experiments.

Inhibition of p38 MAPK ameliorated hypoxia-induced fibrosis.

Further, the role of p38 MAPK inhibition was demonstrated using *in vivo* and *in vitro* models. First, phospho-p38 MAPK expressions in the kidney tissue and kidney mRNA were measured. The enhanced tissue expressions of phospho-p38 MAPK in WT mice compared to those in control mice were substantially decreased in *Postn null* mice as shown by immunohistochemistry assays (**Figure 4A**) and immunofluorescence staining (**Figure 4B**).

Consistent with these findings, the mRNA level of p38 MAPK was significantly elevated in WT mice compared to that in control mice and was significantly decreased in *Postn null* mice (WT sham *vs.* WT UIRI *vs.* *Postn null* UIRI 1.14 ± 0.50 *vs.* 5.16 ± 8.72 *vs.* 1.79 ± 1.16; $P < 0.0001$, $P = 0.006$) (**Figure 4C**).

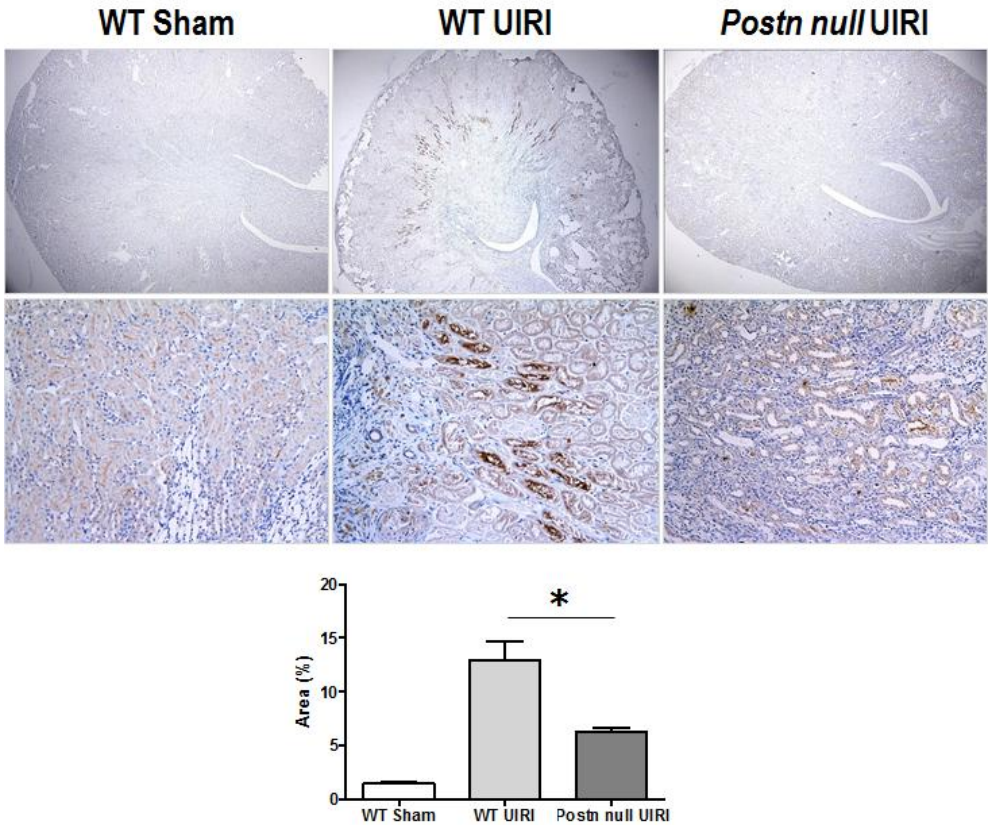

Figure 4. Inhibition of p38 MAPK ameliorated hypoxia-induced fibrosis. (A) The expression of phospho-p38 MAPK in immunohistochemistry. For *in vivo* studies, intrarenal phospho-p38 MAPK expression enhanced in WT mice was substantially ameliorated in *Postn null* mice (n = 8/group; **P* < 0.05; magnification: ×40 (upper panel), ×200 (lower panel)).

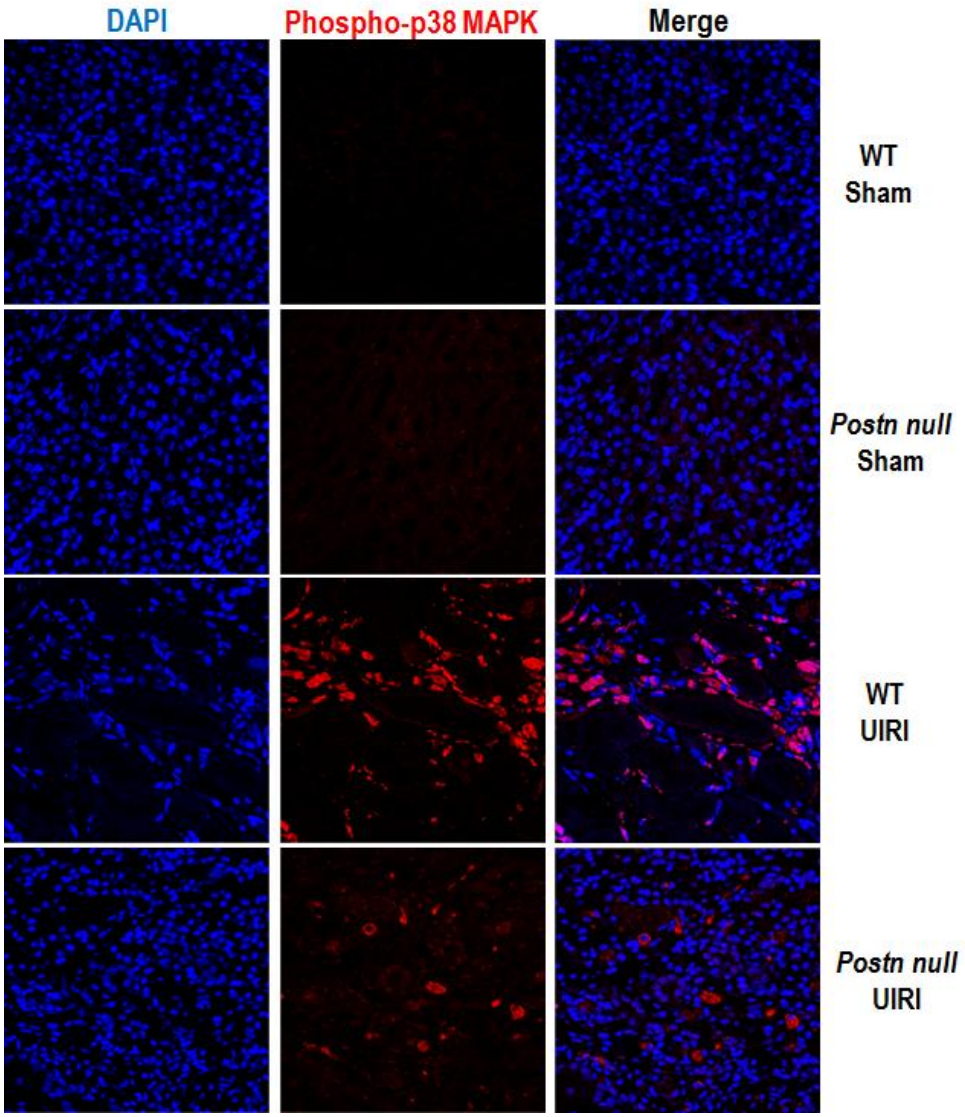

(B) The expression of phospho-p38 MAPK in immunofluorescence staining. Tissue phospho-p38 MAPK expression enhanced in WT mice was ameliorated in *Postn null* mice as determined by immunofluorescence staining (n = 8/group; magnification: ×800).

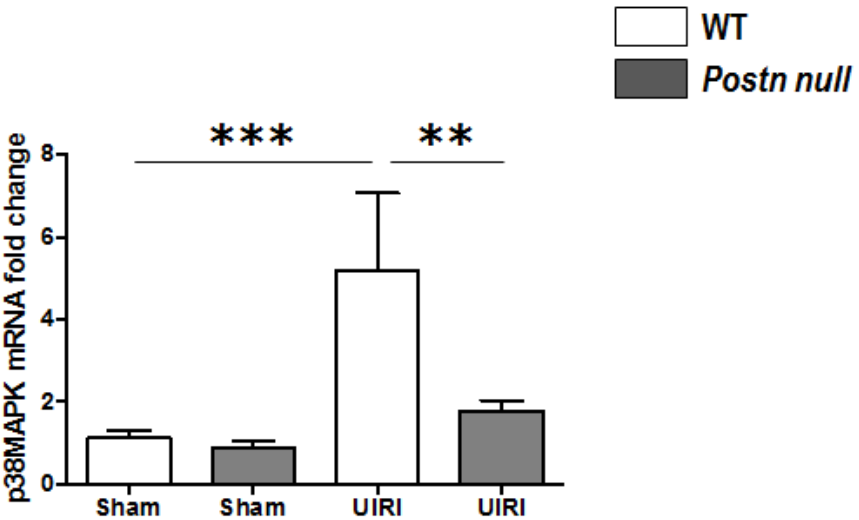

(C) The expression of p38 MAPK in real-time PCR. The mRNA level of p38 MAPK was significantly elevated in WT mice compared to that in control mice and was, significantly decreased in *Postn null* mice (n = 10/group; $^{**}P < 0.01$, $^{***}P < 0.001$) Data are shown as mean ± standard deviation and Student's t-test was used. These results represent one of three independent experiments.

Second, for *in vitro* studies, the early expression of phospho-p38 MAPK was confirmed through confocal microscopic examination (**Figure 5A**). The HK-2 cells incubated in hypoxic conditions for 24 hours increased phospho-p38 MAPK expression, which was similar to the results following treatment with rTGF-β1 under normoxic conditions. Furthermore, hypoxia in combination with rPeriostin significantly magnified the expression of phospho-p38 MAPK, which was also comparable to that following treatment with rTGF-β1 under hypoxia.

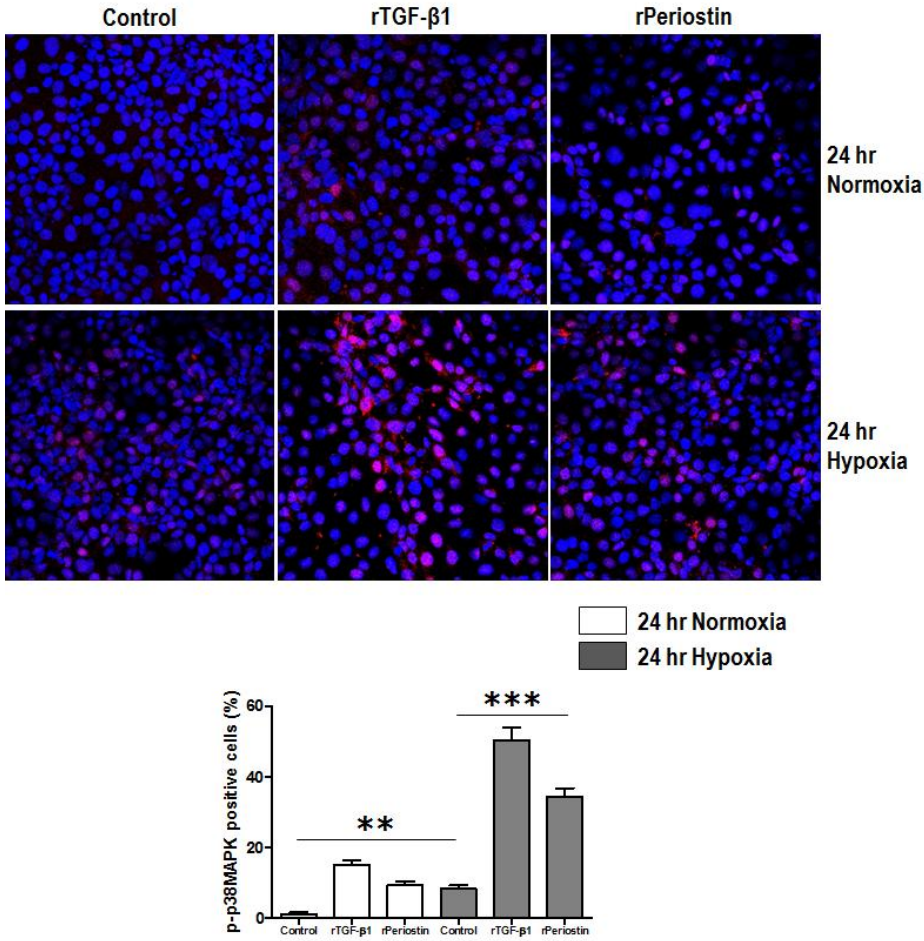

Figure 5. For *in vitro* studies, the effects of p38 MAPK inhibition. (A) The expression of phospho-p38 MAPK in HK-2 cells. For *in vitro* studies, hypoxia injury for 24 hours resulted in phospho-p38 MAPK expression, which was comparable to that with rTGF-β1 under normoxia. In addition, the expression of phospho-p38 MAPK under hypoxia was substantially augmented by the administration of rPeriostin, which was comparable to that with rTGF-β1 under hypoxia (**$P < 0.01$, ***$P < 0.001$; magnification: ×800).

Finally, to confirm the hypothesis that p38 MAPK inhibition affected fibrosis markers, HK-2 cells cultured with rTGF-β1 at normoxic condition and with a p38 MAPK inhibitor at hypoxic condition were harvested after 5 days. Hypoxia injury enhanced the fibronectin, collagen 1A1, α-SMA, periostin, and snail expressions comparable to or much greater than those following treatment with rTGF-β1 under normoxia; however, these expressions were substantially mitigated by the use of the p38 MAPK inhibitor (dose-dependent). In contrast, decreased E-cadherin expression under hypoxia injury was significantly augmented by p38 MAPK inhibition (**Figure 5B)**.

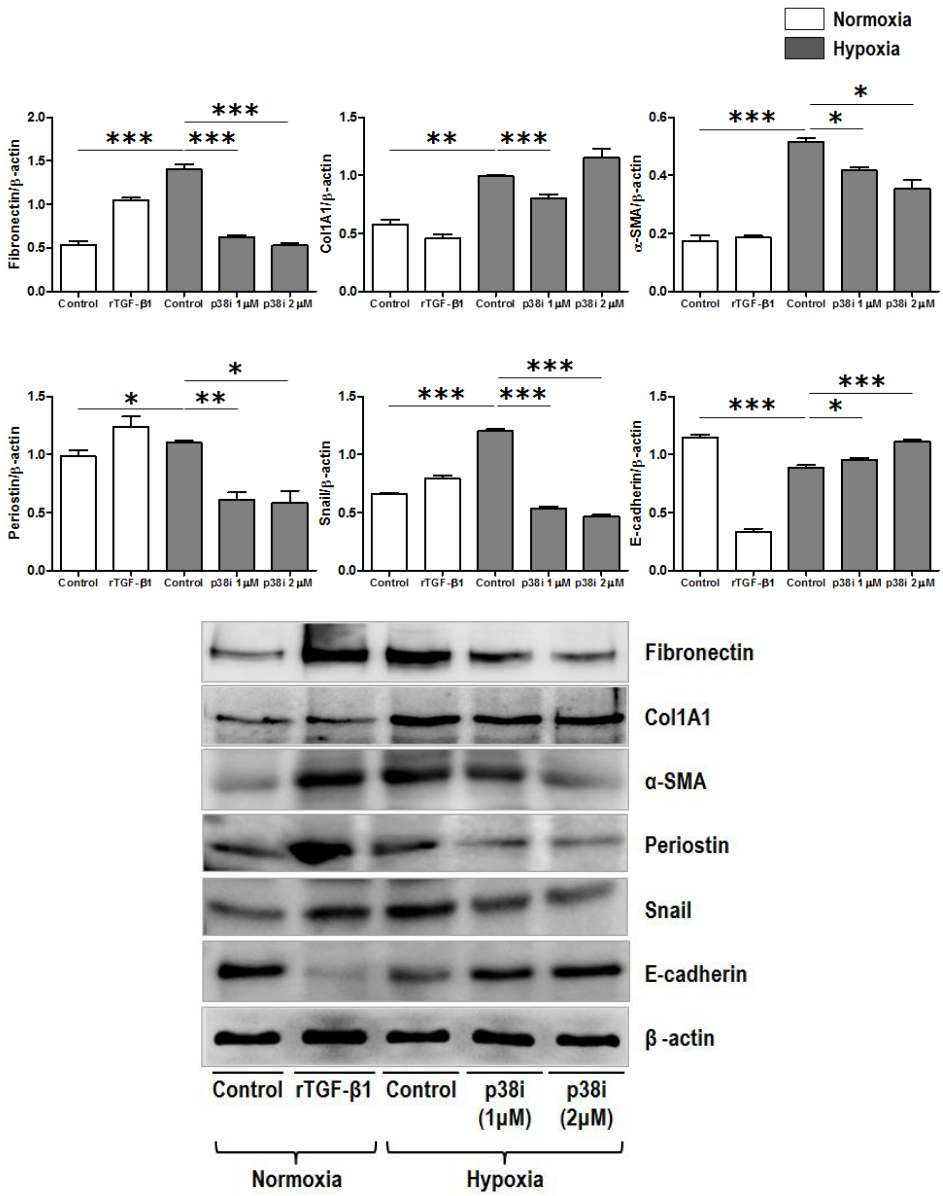

(B) Western blot analysis. HK-2 cells were cultured with rTGF-β1 at normoxic conditions and with a p38 MAPK inhibitor in hypoxic conditions. After 5 days, the expression of fibronectin, collagen 1A1, α-SMA, periostin, and snail following hypoxia injury were observed, which were comparable to or much greater than that

with rTGF-β1 treatment under normoxia. However, the addition of the p38 MAPK inhibitor markedly alleviated these changes. Decreased expression of E-cadherin under hypoxia was increased by p38 MAPK inhibition. (*P < 0.05, **P < 0.01, ***P < 0.001). Data are shown as mean ± standard deviation and Student's t-test was used. These results represent one of three independent experiments. After densitometry analyses of the results of western blot analyses for all cellular protein samples, the results of representative samples are shown in the figure.

Discussion

In this study, an experimental model of the progression from AKI to CKD was established and the association between periostin and this model was investigated. The protective effects of periostin suppression and a correlation with the p38 MAPK pathway were also identified.

The unilateral IRI *in vivo* model established in this study represented the progression to CKD after 6 weeks following AKI induced by ischemia and hypoxic injury, which has become an important issue recently [28]. This experimental model is relevant due to the clinical importance of progression from AKI to CKD.

In a previous study, periostin mRNA expression in tissues was expressed in inverse proportion to renal function of the patients with various kidney diseases accompanied with tubulo-interstitial fibrosis or glomerular injury [12]. In addition, the mRNA level of periostin was significantly associated with proteinuria, serum Cr level, and renal blood flow in a hypertensive nephropathy rat model [14]. Bancha et al. also demonstrated the expression of periostin in 5/6 nephrectomy, streptozotocin-induced diabetic nephropathy, and unilateral ureteral obstruction *in vivo* models [29]. For the *in vitro* model using human collecting duct cells, periostin was also highly expressed following rTGF-β1 administration in a dose-dependent manner, and periostin increased the expression of collagen 1A1 [30].

Most recently, it was found that urine periostin levels were correlated with renal pathologies and longer-term renal outcomes in patients with IgA nephropathy [31]. Similarly, the finding that periostin was closely related to renal function and tissue fibrosis, has been confirmed in the human samples and in the newly established fibrosis model (progressive kidney injury model).

Furthermore, this study examined the protective effects of periostin

suppression through experiments using the *Postn null* mice. The effects of periostin suppression have been reported by several studies. Cultured mouse distal collecting tubular cells transfected with periostin cDNA exhibited increased periostin expression with fibrosis induction; however, those treated with periostin siRNA showed attenuation of fibrosis [29]. Most recently, in a unilateral ureteral obstruction *in vivo* model using *Postn null* mice [30], fibrosis was significantly alleviated compared to that in WT mice.

In this study, the unilateral IRI model using *Postn null* mice showed that the changes in gross appearance, fibrosis, and apoptosis were less severe compared with those of the WT mice. Through these findings, the protective effect of periostin suppression on the progression of AKI to CKD was verified. These results were also consistent with those of Oka et al., who reported that *Postn null* mice exhibited less severe infiltration of fibroblasts and scarring of left ventricle following myocardial infarction, and better long-term cardiac function than those in WT mice [32].

Meanwhile, the association between the p38 MAPK pathway and periostin in the progression of AKI to CKD was investigated. p38 MAPK, a serine/threonine kinase, regulates several cellular activities including gene expression, mitosis, differentiation, migration, survival, and apoptosis in response to extracellular stimulation. It is activated by pro-inflammatory cytokines, pathogens, growth factors, and environmental factors such as hypoxia, ischemia, and reactive oxygen species; therefore, it plays an important role in initiation and progression of inflammatory reactions. The p38 MAPK cascade is primarily found in macrophages, endothelial cells, myocardial cells, and renal cells [33-37]. Previous studies have shown the effect of activation or suppression of p38 MAPK on various diseases.

Suppression of p38 MAPK decreased inflammation and necrosis, and improved microvascular function and coronary blood flow, which resulted in an improvement in interstitial and perivascular fibrosis [38, 39]. In an

ischemia-reperfusion injury model, proteinuria, acute tubular necrosis, and finally kidney fibrosis and mortality decreased following administration of a p38 MAPK inhibitor [34, 40, 41]. Moreover, several kidney disease models [35, 36] demonstrated that p38 MAPK inhibition caused prominent alleviation of renal function decline, proteinuria, inflammation, glomerular sclerosis, and interstitial fibrosis.

Consistent with these findings, the present study demonstrated an increase in phospho-p38 MAPK after disease induction in both *in vivo* and *in vitro* models, and a dose-dependent decrease in fibrosis markers following addition of a p38 MAPK inhibitor. These findings indicated a crucial role of p38 MAPK in fibrosis due to hypoxia and ischemia injury and that the effects of periostin were related to the p38 MAPK pathway, given the decreased expression of phospho-p38 MAPK in *Postn null* mice.

Several limitations to this study should be noted. First, the effects of a p38 MAPK inhibitor were not examined for *in vivo* study. However, hypoxia-induced fibrosis using the *in vitro* model clearly demonstrated the effects of p38 MAPK inhibition on progressive kidney injury. Second, the differences and changes over time were not investigated for the *in vivo* model; however, in preliminary experiments, increased expression of periostin was found after 2 days of bilateral IRI induction, which was conventional AKI *in vivo* model. Third, the in-depth mechanisms underlying the association between periostin and the p38 MAPK pathway in the progression of AKI to CKD were not elucidated. Ultimately, further studies regarding these mechanisms should be performed.

Nevertheless, this study first established the correlation between periostin/periostin suppression and a progressive kidney injury model through changes in fibrosis or apoptosis, and by extension, confirmed the dose-dependent effects of p38 MAPK inhibition in *in vitro* study. In conclusion, periostin was related to the progression to kidney fibrosis via the

p38 MAPK pathway following acute kidney injury triggered by hypoxic or ischemic insult. Periostin ablation could have protective effects on kidney progression.

References

1. Kruzynska-Frejtag A, Machnicki M, Rogers R, et al. Periostin (an osteoblast-specific factor) is expressed within the embryonic mouse heart during valve formation. *Mech Dev.* 2001;103:183-188.

2. Norris RA, Kern CB, Wessels A, et al. Identification and detection of the periostin gene in cardiac development. *Anat Rec A Discov Mol Cell Evol Biol.* 2004;281:1227-1233.

3. Kii I, Amizuka N, Minqi L, et al. Periostin is an extracellular matrix protein required for eruption of incisors in mice. *Biochem Biophys Res Commun.* 2006;342:766-772.

4. Asakura M, Kitakaze M. Global gene expression profiling in the failing myocardium. *Circ J.* 2009;73:1568-1576.

5. Zhao S, Wu H, Xia W, et al. Periostin expression is upregulated and associated with myocardial fibrosis in human failing hearts. *J Cardiol.* 2014;63:373-378.

6. Dobaczewski M, Gonzalez-Quesada C, Frangogiannis NG. The extracellular matrix as a modulator of the inflammatory and reparative response following myocardial infarction. *J Mol Cell Cardiol.* 2010;48:504-511.

7. Ling L, Cheng Y, Ding L, et al. Association of serum periostin with cardiac function and short-term prognosis in acute myocardial infarction patients. *PLoS One.* 2014;9:e88755.

8. Jia G, Erickson RW, Choy DF, et al. Periostin is a systemic biomarker of eosinophilic airway inflammation in asthmatic patients. *J Allergy Clin Immunol.* 2012;130:647-654 e610.

9. Kudo Y, Siriwardena BS, Hatano H, et al. Periostin: novel diagnostic and therapeutic target for cancer. *Histol Histopathol.* 2007;22:1167-1174.

10. Ruan K, Bao S, Ouyang G. The multifaceted role of periostin in tumorigenesis. *Cell Mol Life Sci.* 2009;66:2219-2230.

11. Underwood TJ, Hayden AL, Derouet M, et al. Cancer-associated fibroblasts predict poor outcome and promote periostin-dependent invasion in oesophageal adenocarcinoma. *J Pathol.* 2015;235:466-477.

12. Sen K, Lindenmeyer MT, Gaspert A, et al. Periostin is induced in glomerular injury and expressed de novo in interstitial renal fibrosis. *Am J Pathol.* 2011;179:1756-1767.

13. Braun N, Sen K, Alscher MD, et al. Periostin: a matricellular protein involved in peritoneal injury during peritoneal dialysis. *Perit Dial Int.* 2013;33:515-528.

14. Guerrot D, Dussaule JC, Mael-Ainin M, et al. Identification of periostin as a critical marker of progression/reversal of hypertensive nephropathy. *PLoS One.* 2012;7(3):e31974.

15. Morra L, Moch H. Periostin expression and epithelial-mesenchymal transition in cancer: a review and an update. *Virchows Arch.* 2011;459:465-475.

16. Horiuchi K, Amizuka N, Takeshita S, et al. Identification and characterization of a novel protein, periostin, with restricted expression to periosteum and periodontal ligament and increased expression by transforming growth factor beta. *J Bone Miner Res.* 1999;14:1239-1249.

17. Norris RA, Moreno-Rodriguez R, Hoffman S, et al. The many facets of the matricelluar protein periostin during cardiac development, remodeling, and pathophysiology. *J Cell Commun Signal.* 2009;3:275-286.

18. Roberts DD. Emerging functions of matricellular proteins. *Cell Mol Life Sci.* 2011;68:3133-3136.

19. Hsu RK, McCulloch CE, Dudley RA, et al. Temporal changes in

incidence of dialysis-requiring AKI. *J Am Soc Nephrol.* 2013;24:37-42.

20. Nash K, Hafeez A, Hou S. Hospital-acquired renal insufficiency. *Am J Kidney Dis.* 2002;39:930-936.

21. Chertow GM, Burdick E, Honour M, et al. Acute kidney injury, mortality, length of stay, and costs in hospitalized patients. *J Am Soc Nephrol.* 2005;16:3365-3370.

22. Pannu N, James M, Hemmelgarn B, et al. Association between AKI, recovery of renal function, and long-term outcomes after hospital discharge. *Clin J Am Soc Nephrol.* 2013;8:194-202.

23. Chawla LS, Amdur RL, Amodeo S, et al. The severity of acute kidney injury predicts progression to chronic kidney disease. *Kidney Int.* 2011;79:1361-1369.

24. Thakar CV, Christianson A, Himmelfarb J, et al. Acute kidney injury episodes and chronic kidney disease risk in diabetes mellitus. *Clin J Am Soc Nephrol.* 2011;6:2567-2572.

25. An JN, Hwang JH, Kim DK, et al. Chronic Kidney Disease After Acute Kidney Injury Requiring Continuous Renal Replacement Therapy and Its Impact on Long-Term Outcomes: A Multicenter Retrospective Cohort Study in Korea. *Crit Care Med.* 2017;45:47-57.

26. Rios H, Koushik SV, Wang H, et al. periostin null mice exhibit dwarfism, incisor enamel defects, and an early-onset periodontal disease-like phenotype. *Mol Cell Biol.* 2005;25:11131-11144.

27. Page TH, Brown A, Timms EM, et al. Inhibitors of p38 suppress cytokine production in rheumatoid arthritis synovial membranes: does variable inhibition of interleukin-6 production limit effectiveness in vivo? *Arthritis Rheum.* 2010;62:3221-3231.

28. Le Clef N, Verhulst A, D'Haese PC, et al. Unilateral Renal Ischemia-Reperfusion as a Robust Model for Acute to Chronic

Kidney Injury in Mice. *PLoS One.* 2016;11:e0152153.

29. Satirapoj B, Wang Y, Chamberlin MP, et al. Periostin: novel tissue and urinary biomarker of progressive renal injury induces a coordinated mesenchymal phenotype in tubular cells. *Nephrol Dial Transplant.* 2012;27:2702-2711.

30. Mael-Ainin M, Abed A, Conway SJ, et al. Inhibition of periostin expression protects against the development of renal inflammation and fibrosis. *J Am Soc Nephrol.* 2014;25:1724-1736.

31. Hwang JH, Lee JP, Kim CT, et al. Urinary Periostin Excretion Predicts Renal Outcome in IgA Nephropathy. *Am J Nephrol.* 2016;44:481-492.

32. Oka T, Xu J, Kaiser RA, et al. Genetic manipulation of periostin expression reveals a role in cardiac hypertrophy and ventricular remodeling. *Circ Res.* 2007;101:313-321.

33. Lee JC, Kumar S, Griswold DE, et al. Inhibition of p38 MAP kinase as a therapeutic strategy. *Immunopharmacology.* 2000;47:185-201.

34. Furuichi K, Wada T, Iwata Y, et al. Administration of FR167653, a new anti-inflammatory compound, prevents renal ischaemia/reperfusion injury in mice. *Nephrol Dial Transplant.* 2002;17:399-407.

35. Stambe C, Atkins RC, Tesch GH, et al. Blockade of p38alpha MAPK ameliorates acute inflammatory renal injury in rat anti-GBM glomerulonephritis. *J Am Soc Nephrol.* 2003;14:338-351.

36. Li J, Campanale NV, Liang RJ, et al. Inhibition of p38 mitogen-activated protein kinase and transforming growth factor-beta1/Smad signaling pathways modulates the development of fibrosis in adriamycin-induced nephropathy. *Am J Pathol.* 2006;169:1527-1540.

37. Tenhunen O, Rysa J, Ilves M, et al. Identification of cell cycle

regulatory and inflammatory genes as predominant targets of p38 mitogen-activated protein kinase in the heart. *Circ Res.* 2006;99:485-493.

38. Ma XL, Kumar S, Gao F, et al. Inhibition of p38 mitogen-activated protein kinase decreases cardiomyocyte apoptosis and improves cardiac function after myocardial ischemia and reperfusion. *Circulation.* 1999;99:1685-1691.

39. Li Z, Ma JY, Kerr I, et al. Selective inhibition of p38alpha MAPK improves cardiac function and reduces myocardial apoptosis in rat model of myocardial injury. *Am J Physiol Heart Circ Physiol.* 2006;291:H1972-1977.

40. Jayle C, Faure JP, Thuillier R, et al. Influence of nephron mass and a phosphorylated 38 mitogen-activated protein kinase inhibitor on the development of early and long-term injury after renal warm ischaemia. *Br J Surg.* 2009;96:799-808.

41. Cau J, Favreau F, Zhang K, et al. FR167653 improves renal recovery and decreases inflammation and fibrosis after renal ischemia reperfusion injury. *J Vasc Surg.* 2009;49:728-740.

국문요약

Periostin이 급성신손상 후 신 섬유화에 미치는 영향

안 정 남
임상의과학과 전공
서울대학교 대학원

서론: 페리오스틴은 모세포 단백질(matricellular protein) 중 하나로 섬유화 과정에 중요한 역할을 한다고 알려져 있다. 급성신손상은 만성콩팥병 진행의 중요한 위험 인자이다. 본 연구에서는 급성신손상이 신 섬유화로 진행하는데 있어 페리오스틴이 관여한다는 가설을 세웠다.

방법: 동물실험으로, 7-8 주령의 수컷 표준형(wild-type) 마우스와 페리오스틴 결핍(*periostin null*) 마우스를 이용하여 일측성 허혈-재관류 손상을 유도하였고, 6주 동안 관찰하였다. 생체 외 실험을 위해, 사람 신장-2 (human kidney-2) 세포를 저산소 세포 배양기(5% O_2, 5% CO_2, and 90% N_2)에 넣어 24시간과 5일 동안 배양하였다. 일부 세포에는 p38 미토겐 활성화 단백질 키나아제(mitogen-activated protein kinase, MAPK) 억제제를 처리하여 5일간 배양하였다.

결과: 일측성 허혈-재관류 손상을 유도하고 6주 후, 표준형 마우스에 비하여 *periostin null* 마우스의 좌측 신장은 덜 위축되었고 세뇨관 위축성 변화와 간질 섬유화도 유의하게 완화되었다. 또한, 표준형 마우스와 비교하였을 때, *periostin null* 마우스에서 phosphorylated p38 MAPK의 발현이 유의하게 감소하였을 뿐 아니라, 다양한 섬유화 및 세포자멸(apoptosis) 마커들의 mRNA와 단백 발현이 약화되는 것을 확인하였다.

생체 외 실험에서는, 사람 신장-2 세포에 각각 24시간과 5일 동안 저산소 자극(5% O_2, 5% CO_2, and 90% N_2)을 주었을 때, phospho-p38 MAPK 및 다양한 섬유화 마커의 발현이 증가함을 확인하였다. 저산소 상태에서 재조합 페리오스틴을 처리하였을 때 phospho-p38 MAPK 발현이 더 증가하였는데, 이는 재조합 transforming growth factor-β1을 처리하였을 때의 결과와 비슷한 정도였다. 반면, p38 MAPK를 억제하였을 때는 저산소 유도 섬유화가 개선되는 결과를 보였다.

결론: 결론적으로, 페리오스틴은 저산소증 및 허혈성 자극에 의한 급성 신손상 후 동반되는 신 섬유화 진행에 관여하며 이는 p38 MAPK 경로와 연관되어 있다. 페리오스틴을 억제하는 것은 신 섬유화 진행에 예방 효과(protective effect)를 가지는 것으로 생각된다.

주요어: 페리오스틴, 급성신손상, 신 섬유화, 저산소증, *periostin null* mice, 일측성 허혈-재관류 손상, p38 mitogen-activated protein kinase

학 번: 2014-30912